1521-009X/12/4001-159–168$25.00
DRUG METABOLISM AND DISPOSITION
Vol. 40, No. 1
42200/3739871
DMD 40:159–168, 2012

Prediction of Relative In Vivo Metabolite Exposure from In Vitro Data Using Two Model Drugs: Dextromethorphan and Omeprazole

Justin D. Lutz and Nina Isoherranen

Department of Pharmaceutics, University of Washington School of Pharmacy, Seattle, Washington

Received August 5, 2011; accepted October 18, 2011

ABSTRACT:

Metabolites can have pharmacological or toxicological effects, inhibit metabolic enzymes, and be used as probes of drug-drug interactions or specific cytochrome P450 (P450) phenotypes. Thus, better understanding and prediction methods are needed to characterize metabolite exposures in vivo. This study aimed to test whether in vitro data could be used to predict and rationalize in vivo metabolite exposures using two model drugs and P450 probes: dextromethorphan and omeprazole with their primary metabolites dextrorphan, 5-hydroxyomeprazole (5OH-omeprazole), and omeprazole sulfone. Relative metabolite exposures were predicted using metabolite formation and elimination clearances. For dextrorphan, the formation clearances of dextrorphan glucuronide and 3-hydroxymorphinan from dextrorphan in human liver microsomes were used to predict metabolite (dextrorphan) clearance. For 5OH-omeprazole and omeprazole sulfone, the depletion rates of the metabolites in human hepatocytes were used to predict metabolite clearance. Dextrorphan/dextromethorphan in vivo metabolite/parent area under the plasma concentration versus time curve ratio (AUC_m/AUC_p) was overpredicted by 2.1-fold, whereas 5OH-omeprazole/omeprazole and omeprazole sulfone/omeprazole were predicted within 0.75- and 1.1-fold, respectively. The effect of inhibition or induction of the metabolite's formation and elimination on the AUC_m/AUC_p ratio was simulated. The simulations showed that unless metabolite clearance pathways are characterized, interpretation of the metabolic ratios is exceedingly difficult. This study shows that relative in vivo metabolite exposure can be predicted from in vitro data and characterization of secondary metabolism of probe metabolites is critical for interpretation of phenotypic data.

Introduction

Metabolites of drugs can possess in vivo pharmacologic, toxicologic, or enzyme inhibitory activity and contribute to the clinical effects of the drug (Ho et al., 2003; Riss et al., 2008). For example, the secondary metabolite of clopidogrel, (3*Z*)-3-(carboxymethylene)-α-(2-chlorophenyl)-4-mercapto-1-piperidineacetic acid 1-methyl ester (R-130964), is the primary active species that is responsible for the anticoagulant effect in vivo, and decreasing its abundance in vivo leads to decreased pharmacological effect (Angiolillo et al., 2011). The role of metabolites in drug toxicity is illustrated by the removal of fenfluramine from the U.S. market because of its association with valvular heart disease. This cardiovascular toxicity was proposed to be 5-HT_{2B} receptor-mediated, and norfenfluramine, the *N*-deethylated metabolite of fenfluramine, was demonstrated to be a significantly more potent agonist of human 5-HT_{2B} receptors than fenfluramine (Fitzgerald et al., 2000). The inhibition of cytochrome P450 (P450) 2D6 after bupropion administration seems to be mainly due to the primary metabolites of bupropion rather than bupropion itself, demonstrating the potential role of metabolites in inhibitory drug-drug interactions (Reese et al., 2008; Yeung et al., 2011). Because of the concern of exposures to metabolites in humans that are not covered by preclinical safety testing, the U.S. Food and Drug Administration and the European Medicines Agency recently published guidance documents for the safety testing of metabolites (www.fda.gov/downloads/Drugs/GuidanceComplianceRegulatoryInformation/Guidances/ucm079266.pdf and www.ema.europa.eu/pdfs/human/ich/028695en.pdf), and the European Medicines Agency included recommendations for in vitro P450 enzyme inhibition testing of new drug metabolites (http://www.ema.europa.eu/ema/pages/includes/document/open_document.jsp?webContentId = WC500090112). These recent guidance documents have drawn attention to the development of methods for early identification of metabolites and prediction of metabolite exposures (Anderson et al., 2009; Leclercq et al., 2009).

This work was supported by the National Institutes of Health National Institute of General Medical Sciences [Grant P01-GM32165-02].

Article, publication date, and citation information can be found at http://dmd.aspetjournals.org.

http://dx.doi.org/10.1124/dmd.111.042200.

ABBREVIATIONS: R-130964, (3*Z*)-3-(carboxymethylene)-α-(2-chlorophenyl)-4-mercapto-1-piperidineacetic acid 1-methyl ester; 5-HT, 5-hydroxytryptamine; P450, cytochrome P450; 5OH-omeparazole, 5-hydroxyomeprazole; AUC, area under the plasma concentration versus time curve; AUC_m/AUC_p, metabolite/parent area under the plasma concentration versus time curve ratio; BSA, bovine serum albumin; Cl, clearance; Cl_f, metabolite formation clearance; Cl_i, intrinsic clearance; $Cl_{i,dep}$, intrinsic depletion clearance; $Cl_{i,f}$, metabolite intrinsic formation clearance; $Cl_{i,u}$, intrinsic unbound clearance; C_m/C_p, metabolite/parent plasma concentration ratio; E, enzyme; f_u, fraction unbound; $f_{u,mic}$, microsomal fraction unbound; HLM, human liver microsomes; KPi, potassium phosphate; M, metabolite; MP, microsomal protein; P, parent; rUGT, recombinantly expressed uridine diphosphate glucuronosyltransferase; UDPGA, uridine diphosphate glucuronic acid; UGT, uridine diphosphate glucuronosyltransferase; V_{max}, maximum velocity; HPLC, high-performance liquid chromatography; ADH, alcohol dehydrogenase.

Metabolic ratios such as the metabolite/parent area under the plasma concentration versus time curve ratio (AUC_m/AUC_p), plasma concentration of the metabolite/parent ratio (C_m/C_p), or urinary concentration ratios are commonly used in drug-drug interaction and pharmacogenetic studies as in vivo activity measures of the P450 mediating the formation of the metabolite. Use of metabolite formation or a metabolic ratio instead of an area under the plasma concentration versus time curve (AUC) of the parent drug is necessary when the parent drug is only partially cleared by the P450 isoform of interest. Commonly used metabolic ratios include the hydroxybupropion/bupropion ratio for CYP2B6, the paraxanthine/caffeine ratio for CYP1A2, the dextrorphan/dextromethorphan ratio for CYP2D6, and the 5-hydroxyomeprazole/omeprazole ratio for CYP2C19 (Jones et al., 1996; Streetman et al., 2000; Yu and Haining, 2001; Abduljalil et al., 2010). The 3-methoxymorphinan/dextromethorphan and omeprazole sulfone/omeprazole ratios have also been proposed as CYP3A4 probes (Jones et al., 1996; Bertilsson et al., 1997; Böttiger et al., 1997; Tu et al., 2010). In general, a decrease in the metabolic ratio is interpreted as inhibition of the P450 forming the metabolite or a poor metabolizer phenotype, whereas an increase suggests induction of the specific metabolic pathway. All metabolite/parent ratios are dependent on the formation and elimination clearances of the metabolite, and their interpretation relies on the assumption that the clearance of the metabolite is not affected by the treatment or the genotype studied (Levy et al., 1983). However, the elimination pathways and relative contribution of specific enzymes for the clearance of the metabolite may be inadequately characterized, and the effect of interacting drug on the probe metabolite clearance is rarely determined. Hence, the interpretation of the metabolic ratio may be confounded by changes in metabolite clearance.

A method for predicting the in vivo metabolite/parent AUC_m/AUC_p using clearance scaling from in vitro metabolite formation and elimination data was proposed and tested using literature data for six metabolite/parent pairs (Lutz et al., 2010). The proposed method could be useful for a priori prediction of the relative metabolite exposure in vivo before clinical testing, or for identification of important secondary metabolism of metabolites whose AUC_m/AUC_p are greatly overpredicted after clinical administration. To test the method, published in vitro data for the formation of 3-hydroxymorphinan from dextrorphan (Fig. 1) (Kerry et al., 1994) and of 5-hydroxyomeprazole sulfone from 5-hydroxyomeprazole (5OH-omeprazole) (Fig. 2) (Andersson et al., 1993, 1994) were used to predict in vivo AUC_m/AUC_p ratios for dextrorphan/dextromethorphan and 5OH-omeprazole/omeprazole. The metabolite/parent AUC ratios were overpredicted by 160- and 20-fold for dextrorphan/dextromethorphan and 5OH-omeprazole/omeprazole, respectively, indicating that significant uncharacterized metabolic pathways exist for dextrorphan and 5OH-omeprazole. The aim of this study was to determine whether these elimination pathways do exist and whether the dextrorphan/dextromethorphan, 5OH-omeprazole/omeprazole, and omeprazole sulfone/omeprazole in vivo AUC_m/AUC_p could be accurately predicted using in vitro metabolism data. Finally, the effect of altered secondary metabolism on in vivo AUC_m/AUC_p was tested via pharmacokinetic simulation.

Materials and Methods

Chemicals and Reagents. Dextromethorphan, dextrorphan, 3-hydroxymorphinan, omeprazole, 5OH-omeprazole, omeprazole sulfone, NADPH, uridine diphosphate glucuronic acid (UDPGA), alamethicin, and saccharolactone were purchased from Sigma-Aldrich (St. Louis, MO). Dextrorphan-*O*-glucuronide and omeprazole-d_3 were purchased from Toronto Research Chemicals Inc. (North York, ON, Canada). HPLC/mass spectrometry-grade water, acetonitrile, and methanol were purchased from Fisher Scientific (Pittsburgh, PA).

Human Liver Microsome and Recombinantly Expressed UDP-Glucuronosyltransferase Incubations. All human liver microsomes (HLM) incubations were performed using HLM pooled from seven different donors obtained from the University of Washington Human Liver Bank (Seattle, WA). All seven donors were both phenotyped and genotyped to confirm that they were CYP2C19- and CYP2D6-extensive metabolizers and CYP3A5 nonexpressors to avoid potential confounding effects of CYP3A5 expression in metabolite formation and elimination. Recombinantly expressed UDP-glucuronosyltransferase (rUGT) enzymes were obtained from BD Biosciences (San Jose, CA). For all pooled HLM incubations, 0.1 mg of microsomal protein (MP)/ml was used. All P450-mediated incubations were performed in 100 mM potassium phosphate (KPi) buffer at 37°C, after a 10-min preincubation with substrate at 37°C to achieve binding equilibrium. The incubations were then initiated with a 1 mM final concentration of NADPH cofactor. For pooled HLM and rUGT dextrorphan-*O*-glucuronide formation, the incubations were

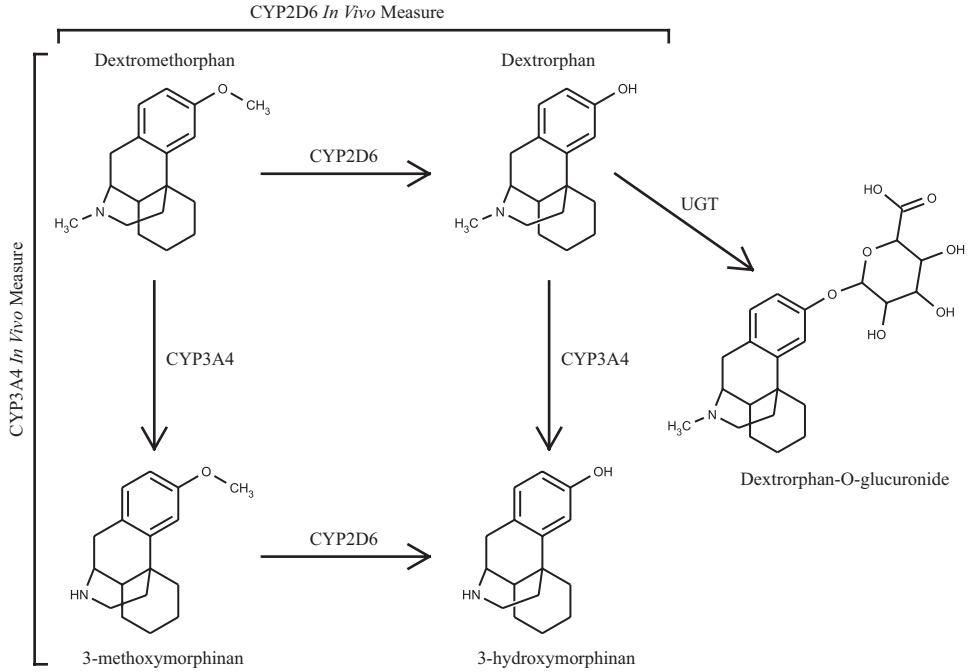

FIG. 1. Metabolic scheme of dextromethorphan. The enzyme responsible for the formation of each metabolite and the metabolite/parent pair used as an in vivo activity measure for the specified P450 isoform is indicated. UGT indicates proposed UDP-glucuronosyltransferase metabolism.

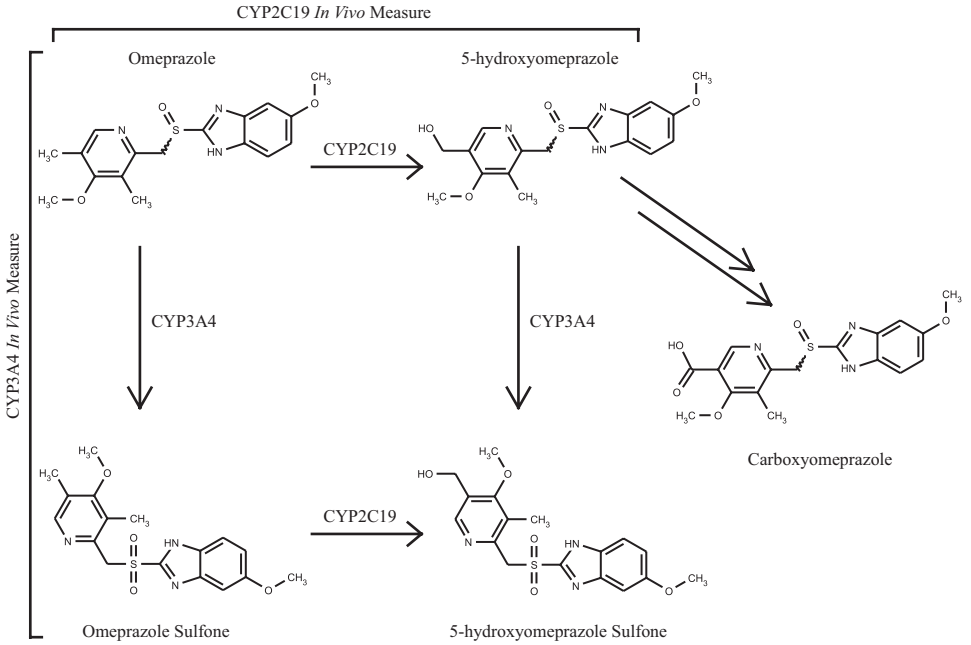

FIG. 2. Metabolic scheme of omeprazole. The enzyme responsible for the formation of each metabolite and the metabolite/parent pair used as an in vivo activity measure for the specified P450 isoform are indicated.

first preincubated with 50 μg/mg MP alamethicin and 5 mM saccharolactone on ice in 100 mM KPi buffer for 30 min to allow insertion of the alamethicin pore former into the microsomal membrane and then further preincubated at 37°C for 10 min to bring the sample to 37°C and to achieve binding equilibrium. The incubations were then initiated with a 5 mM final concentration of UDPGA cofactor. Pooled HLM dextrorphan-*O*-glucuronide formation was performed in the absence and presence of 2% bovine serum albumin (BSA). Except for the substrate depletion experiments, all pooled HLM incubations were performed in 96-well plates in triplicate under determined time and HLM protein linearity conditions. The formation of dextrorphan-*O*-glucuronide by rUGT was measured with 10 μM dextrorphan as the substrate in duplicate. Depletion of 5OH-omeprazole in pooled HLM was determined in the absence and presence of NADPH. The initial concentration of either 5OH-omeprazole or omeprazole sulfone in the substrate depletion experiments was 0.1 μM. All incubations were quenched with equivolume methanol (for dextromethorphan or dextrorphan as the substrate) or acetonitrile (for omeprazole, 5OH-omeprazole, or omeprazole sulfone as the substrate) and centrifuged at 2000*g* for 15 min, and an aliquot was transferred to a clean 96-well plate for analysis.

Human Hepatocyte Incubations. The cryopreserved plated human hepatocyte incubations were performed using a single donor (hu4199) obtained from Invitrogen (Carlsbad, CA). Donor hu4199 was confirmed to exhibit adequate CYP2D6, CYP2C19, and CYP3A4/5 metabolic activity. Hepatocytes were first thawed at 37°C, centrifuged at 100*g* in Cryopreserved Hepatocyte Recovery Media (Invitrogen), and resuspended in plating medium (Dulbecco's modified Eagle's medium containing plating supplements with fetal bovine serum; Invitrogen). Viability and density were measured by trypan blue exclusion, and 52,000 viable cells per well were plated onto 96-well collagen-coated plates. Hepatocytes were allowed to attach for 4 to 6 h, and plating medium was removed and replaced with protein-free maintenance medium (Williams' E medium plus maintenance supplements) containing 0.25 mg/ml Matrigel (BD Biosciences). All hepatocyte incubations were performed in quadruplicate in 96-well plates, using identical protein-free hepatocyte maintenance medium, within 3 days of initial plating. Metabolite formation clearance was determined at 37°C under confirmed time linearity conditions. When determining the hepatocyte formation clearance of either 5OH-omeprazole or omeprazole sulfone, the initial concentration of omeprazole was 1 μM. In the hepatocyte substrate depletion experiments, the initial concentration of either 5OH-omeprazole or omeprazole sulfone was 0.1 μM. All hepatocyte incubations were quenched by the addition of an aliquot of medium into an equal volume of acetonitrile and centrifuged at 2000*g* for 15 min, and an aliquot was transferred to a clean 96-well plate for analysis. The intrinsic formation clearance ($Cl_{i,f}$) of 5OH-omeprazole and omeprazole sulfone from omeprazole was determined over 6 h, and the intrinsic depletion clearance ($Cl_{i,dep}$) of 5OH-omeprazole or omeprazole sulfone was determined over 24 h.

Determination of In Vitro and Plasma Fraction Unbound ($f_{u,mic}$ and f_u, Respectively). A total of 0.1 μM dextromethorphan, dextrorphan, omeprazole, 5OH-omeprazole, or omeprazole sulfone was spiked into either human plasma or HLM at 0.1 mg MP/ml in 100 mM KPi buffer in triplicate. The sample was then divided and either centrifuged at 800,000*g* for 90 min at 37°C or held at 37°C for 90 min without centrifugation, adapted from the method of Templeton et al. (2008). An aliquot was then transferred from both samples to a clean 96-well plate for analysis.

Sample Analysis. Except for dextrorphan-*O*-glucuronide analysis, all pooled HLM incubations were analyzed using a Shimadzu (Kyoto, Japan) HPLC with a CTC autosampler coupled to a Sciex API4000 Q/Q mass spectrometer (Applied Biosystems, Foster City, CA) operating in positive ion electrospray mode. Separation of dextromethorphan and dextromethorphan metabolites was achieved using a Zorbax Eclipse C-18 column (5 μm, 2.1 × 50 mm; Agilent Technologies, Santa Clara, CA) with a solvent gradient (water/methanol) of 80:20 isocratic for 3.5 min, then a linear increase to 45:55 over 2.5 min, and then a rapid increase to and held at 5:95 for 1.5 min. The injection volume was 10 μl. Separation of omeprazole, omeprazole metabolites, and omeprazole-d_3 (internal standard) was achieved using an identical column with a solvent gradient (10 mM ammonium formate in water/acetonitrile) consisting of a linear increase from 95:5 to 65:35 over 6 min and then a hold at 10:90 for 1.5 min. The selected reaction monitoring mass transition, declustering potential (in volts), and collision energy (in volts) values for each analyte are as follows (selected reaction monitoring mass transition, declustering potential, collision energy): dextromethorphan (272 > 171, 60, 50), dextrorphan (258 > 157, 60, 50), 3-hydroxymorphinan (244 > 157, 70, 50), omeprazole (346 > 198, 45, 20), omeprazole-d_3 (349 > 198, 45, 20), 5OH-omeprazole (362 > 214, 55, 20), and omeprazole sulfone (362 > 214, 45, 80). All analyte channels were confirmed to be free of coeluting contaminants, either from the matrix or from other analytes within the assay. The injection volume for both assays was 10 μl. The day-to-day coefficient of variation percentage for all analytes was <15%, and the limits of quantification for all analytes were ≤100 pM.

The formation of dextrorphan-*O*-glucuronide in pooled HLM and rUGTs was analyzed using an Agilent 1100 HPLC and autosampler coupled to an Agilent MSD Q mass spectrometer (Agilent Technologies) operated in negative ion electrospray mode. An identical column to that described above and a solvent gradient (water/methanol) were used with a linear increase from 90:10 to 5:95 over 3 min and held at 5:95 for an additional 3 min. The selected ion

recording mass for dextrorphan-*O*-glucuronide was $[M - H]^- = 432$ *m/z*, and the fragmentor voltage was −5000 V. The injection volume was 10 μl.

The hepatocyte incubations were analyzed using an Infinity 1290 UPLC (Agilent Technologies) coupled to a Sciex API5500 Q/LIT mass spectrometer (Applied Biosystems) operated in positive ion electrospray mode. The separation and detection settings for omeprazole and its metabolites were identical to those described above. The injection volume was 10 μl.

Data Analysis. All data were fit via linear or nonlinear regression numerical analysis using GraphPad Prism version 5 (GraphPad Software Inc., San Diego, CA). Unless noted otherwise, all parameter estimates are given as mean ± S.D. The maximum primary or secondary metabolite formation velocity (V_{max}) and total Michaelis-Menten affinity constant (K_M) in pooled HLM was determined by the following equation:

$$v = \frac{V_{max} \times [S]_0}{K_M + [S]_0} \quad (1)$$

where v and $[S]_0$ are the metabolite formation velocity and initial substrate concentration, respectively. The primary or secondary metabolite total intrinsic formation clearance ($Cl_{i,f}$) was determined by the following equation:

$$Cl_{i,f} = \frac{V_{max}}{K_M} \quad (2)$$

The primary metabolite total intrinsic depletion clearance ($Cl_{i,dep}$) was determined using the following equation:

$$[S]_t = [S]_0 \times e^{\frac{-Cl_{i,dep}}{V_{inc}} \times t} \quad (3)$$

where $[S]_t$ and V_{inc} are the concentration of substrate at a specific time point (t) and the incubation volume, respectively. In hepatocytes, the primary metabolite total intrinsic formation clearance ($Cl_{i,f}$) was determined by the following equation:

$$[M]_t = \frac{Cl_{i,f} \times [S]_0 \times t}{V_{inc}} \quad (4)$$

where $[M]_t$ is the concentration of metabolite at a specific time point. When either $Cl_{i,dep}$ (in pooled HLM and hepatocytes) or $Cl_{i,f}$ (in hepatocytes only) was determined, it was assumed that $[S]_0 \ll K_M$. The pooled HLM fraction unbound ($f_{u,mic}$) or plasma fraction unbound (f_u) for either parent or metabolite was determined by the following equation:

$$f_u = \frac{[A]'}{[A]} \quad (5)$$

where $[A]'$ and $[A]$ are the concentrations of analyte (metabolite or parent) with and without centrifugation, respectively.

Prediction of AUC_m/AUC_p. The in vivo AUC_m/AUC_p for a specific metabolite/parent pair after oral administration was predicted from in vitro data using eqs. 6 and 7.

$$\frac{AUC_m}{AUC_p} = f_{u,p} \times Cl_{f,u} \Big/ \frac{Q_h \times f_{u,m} \times Cl_{m,u}}{Q_h + f_{u,m} \times Cl_{m,u}} \quad (6)$$

Equation 6 assumes that all metabolite formed in the liver is available to the systemic circulation (Lutz et al., 2010). The $f_{u,p}$ and $f_{u,m}$ are the plasma fraction unbound of the parent and metabolite, respectively. The $Cl_{f,u}$ and $Cl_{m,u}$ are the scaled unbound formation and elimination clearances of the metabolite, respectively, and Q_h is hepatic plasma flow. A value of 49.5 l/h was used for Q_h (product of the hepatic blood flow and the proportion of blood that is plasma).

To accommodate likely sequential metabolism of the metabolites within the liver before they reach systemic circulation, eq. 7 was derived. For eq. 7, the formation of the metabolite within the liver is considered analogous to portal vein dosing of the metabolite. Equation 7 is obtained from eq. 6 by adding an additional bioavailability term for the metabolite ($F_h = 1 - ER_h$, where F_h is hepatic bioavailability and ER_h is the hepatic extraction ratio of the metabolite) that represents the fraction of metabolite formed in the liver that is not sequentially metabolized before reaching the systemic circulation (Pang and Gillette, 1979). Incorporation of this metabolite bioavailability term yields eq. 7:

$$\frac{AUC_m}{AUC_p} = \frac{f_{u,p} \times Cl_{i,f}}{f_{u,m} \times Cl_{i,m}} \quad (7)$$

For predictions, all in vitro determined total Cl or Cl_i values were divided by the corresponding $f_{u,mic}$ value to obtain the unbound clearance (Cl_u or $Cl_{i,u}$) values. For all hepatocyte data, the $f_{u,mic}$ was assumed to equal unity, because of the use of protein-free hepatocyte maintenance medium during the incubations. The accuracy of the prediction was determined by the ratio of the predicted value over the observed value, extracted from the literature for in vivo studies that determined both parent and metabolite AUC in plasma. Only in vivo studies in CYP2D6- and CYP2C19-extensive metabolizers as determined by dextromethorphan phenotype or CYP2C19 genotype were used.

Simulations of the Effect of Secondary Metabolism on AUC_m/AUC_p. Using a generic scheme of one enzyme (E1) forming a single metabolite (M) from a parent drug (P) and two enzymes (E1 and E2) eliminating the metabolite, the AUC_m/AUC_p, was simulated using SAAM II (University of Washington, Seattle, WA). It was assumed that the metabolite formed can be sequentially metabolized before reaching the systemic circulation (eq. 7). This simple metabolic scheme is presented as follows:

$$F \times D \xrightarrow{k_a} [P] \xrightarrow{f_{u,p} \times Cl_{f,u}^{E1}} [M] \xrightarrow{f_{u,m} \times (Cl_{m,u}^{E1} + Cl_{m,u}^{E2})}$$

where F, D, and k_a are the bioavailability, dose, and absorption rate constant of the parent after oral administration, respectively. All other variables are as defined previously. Equations 8 and 9 are the differential equations describing the change in parent ($d[P]/dt$) and metabolite ($d[M]/dt$) concentrations over time:

$$\frac{d[P]}{dt} = (F \times D \times k_a - [P] \times f_{u,p} \times X_f^{E1} \times Cl_{f,u}^{E1})/V_p \quad (8)$$

$$\frac{d[M]}{dt} = ([P] \times f_{u,p} \times X_f^{E1} \times Cl_{f,u}^{E1} - [M] \times f_{u,m} \times (X_m^{E1} \times Cl_{m,u}^{E1} + X_m^{E2} \times Cl_{m,u}^{E2}))/V_m \quad (9)$$

where V_p and V_m are the volumes of distribution for the parent and metabolite, respectively. X_f and X_m were incorporated to represent the coefficients describing the effect of induction (>1) or inhibition (<1) on $Cl_{f,u}$ or $Cl_{m,u}$, respectively. All other variables are as defined previously. The second integral of eqs. 8 and 9 describes the AUC_p and AUC_m, respectively. The quotient of AUC_m and AUC_p can be described by eq. 10:

$$\frac{AUC_m}{AUC_p} = \frac{f_{u,p} \times X_f^{E1} \times Cl_{f,u}^{E1}}{f_{u,m} \times (X_m^{E1} \times Cl_{m,u}^{E1} + X_m^{E2} \times Cl_{m,u}^{E2})} \quad (10)$$

The values in eq. 10 were set so that when X_f and X_m were 1, the $AUC_m/AUC_p = 1$. The value for AUC_m/AUC_p was simulated for a range of interactions ($1 \le X \le 10$ for induction and $1 \ge X \ge 0.1$ for inhibition). Several different enzymatic scenarios were considered in which the fraction of metabolite clearance by E1 varied from 0 to 1.

Results

In Vitro Formation and Elimination of Dextrorphan. The formation kinetics of dextrorphan from dextromethorphan was determined in pooled HLM (Fig. 3A). Pooled HLM were also used to characterize 3-hydroxymorphinan and dextrorphan-*O*-glucuronide formation from dextrorphan (Fig. 3, B and C). The kinetic parameters for dextrorphan, 3-hydroxymorphinan, and dextrorphan-*O*-glucuronide formation and the $f_{u,mic}$ and plasma f_u values are summarized in Table 1. The resulting intrinsic clearance for dextrorphan formation from dextromethorphan was 13 μl · min^{-1} · mg MP^{-1} and for 3-hydroxymorphinan formation from dextrorphan was 0.88 μl · min^{-1} · mg MP^{-1}. Dextrorphan-*O*-glucuronide was formed in a

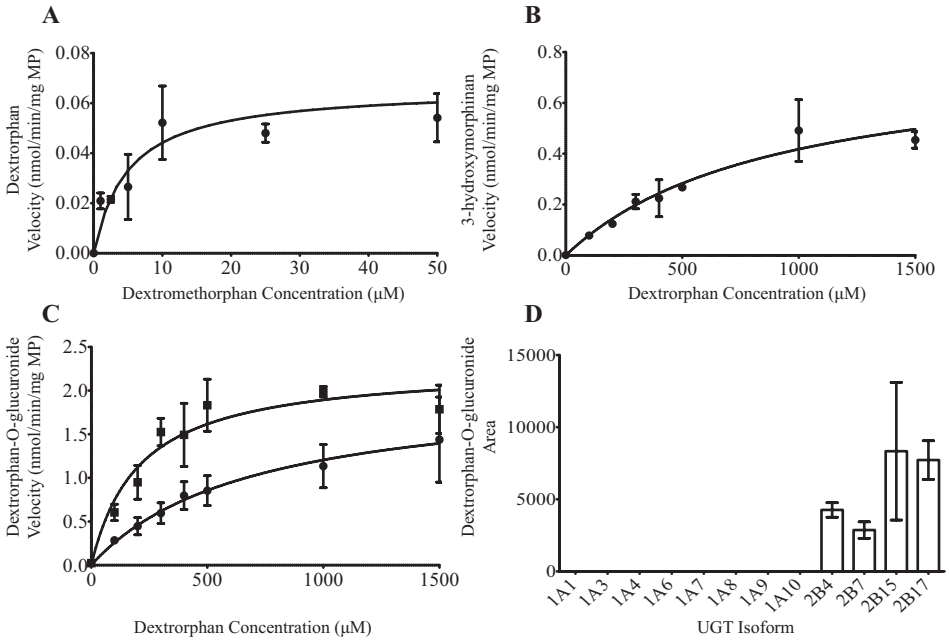

FIG. 3. Characterization of in vitro formation and metabolism of dextrorphan. Formation of dextrorphan from dextromethorphan (A), 3-hydroxymorphinan from dextrorphan (B), and dextrorphan-*O*-glucuronide from dextrorphan (C) in pooled HLM. Dextrorphan-*O*-glucuronide is shown both with (■) and without (●) the presence of 2% BSA. D, formation of dextrorphan-*O*-glucuronide after incubation of dextrorphan with 12 rUGT isoforms. Error bars represent the S.D. of three measurements (A–C) and the range of two measurements (D).

time-, UDPGA cofactor-, and dextrorphan concentration-dependent manner in the presence and absence of 2% BSA. The K_M for dextrorphan glucuronidation determined from total dextrorphan concentration decreased by 70% from 690 ± 140 to 210 ± 110 μM as a result of adding 2% BSA. The $f_{u,mic}$ value for dextrorphan decreased from 1.0 ± 0.04 to 0.88 ± 0.05 in the presence of 2% BSA, and, hence, the unbound K_M decreased from 690 ± 140 to 190 ± 100 μM after addition of 2% BSA. The V_{max} for dextrorphan glucuronidation was unchanged by adding BSA, 2.0 ± 0.2 nmol · min^{-1} · mg MP^{-1} in the absence of BSA, and 2.3 ± 0.4 nmol · min^{-1} · mg MP^{-1} in the presence of BSA. The unbound intrinsic clearance ($Cl_{i,u}$) for dextrorphan-*O*-glucuronide formation was 2.9 μl · min^{-1} · mg MP^{-1} in the absence of BSA and 12 μl · min^{-1} · mg MP^{-1} in the presence of BSA (Table 1). To identify the UGT isoforms responsible for dextrorphan glucuronidation, dextrorphan was incubated with a panel of 12 recombinant UGT isoforms (Fig. 3D). All four UGT2B isoforms studied (2B4, 2B7, 2B15, and 2B17), but none of the eight UGT1A isoforms studied (1A1, 1A3, 1A4, 1A6, 1A7, 1A8, 1A9, and 1A10), formed dextrorphan-*O*-glucuronide, suggesting that dextrorphan glucuronidation is catalyzed mainly by the UGT2B subfamily in vivo.

Prediction of In Vivo Dextrorphan/Dextromethorphan AUC_m/AUC_p. The $Cl_{i,u}$ ($V_{max}/K_{M,u}$) values determined in pooled HLM were scaled to obtain total in vivo formation and elimination clearances (Cl_f and Cl_m, respectively) for dextrorphan. The in vivo AUC_m/AUC_p was predicted using these values and the dextromethorphan and dextrorphan plasma f_u values and compared with in vivo literature values. Using 3-hydroxymorphinan Cl_f from dextrorphan as the only secondary metabolic pathway of dextrorphan yielded a predicted AUC_m/AUC_p of 22 using eq. 6 (all metabolites available for systemic circulation). Because the average observed dextrorphan/dextromethorphan in vivo AUC_m/AUC_p is 0.61 (range, 0.52–0.70), this resulted in an average 36-fold overprediction when compared with published exposure data (Abdul Manap et al., 1999; Yeh et al., 2003; Nakashima et al., 2007). Incorporation of the glucuronidation pathway (characterized in vitro in the presence of 2% BSA) decreased the predicted AUC_m/AUC_p to 2.3 (using eq. 6) and decreased the extent of overprediction to a 3.8-fold average (range, 3.3–4.4) (Table 2). When the glucuronidation pathway of dextrorphan is accounted for, dextrorphan is predicted to be a high-extraction-ratio metabolite, and, hence, it is likely that only a fraction of the formed metabolite is available to systemic circulation. Therefore, eq. 7 was also used for predicting the AUC_m/AUC_p of dextrorphan (Table 2). Indeed, when the glucuronidation characterized in vitro in the presence of 2% BSA and the 3-hydroxymorphinan formation was included, a predicted AUC_m/AUC_p of 1.3 was obtained resulting in an approximately 2-fold overprediction.

In Vitro Formation and Elimination Kinetics of 5OH-Omeprazole and Omeprazole Sulfone. The total intrinsic formation ($Cl_{i,f}$) and elimination ($Cl_{i,dep}$) clearances for 5OH-omeprazole and omeprazole sulfone were determined in pooled HLM and in cryopreserved plated human hepatocytes. Because comprehensive characterization of the secondary metabolites of omeprazole sulfone and 5OH-omepra-

TABLE 1

Kinetic characterization of dextrorphan formation and elimination in human liver microsomes

The Michaelis-Menten constants for the formation of dextrorphan from dextromethorphan and of 3-hydroxymorphinan and dextrorphan-*O*-glucuronide from dextrorphan in HLM are shown. The pooled HLM and plasma unbound fraction values are also listed. The formation of dextrorphan-*O*-glucuronide was determined in the presence and absence of 2% BSA.

	Dextromethorphan→ Dextrorphan	Dextrorphan→ 3-Hydroxymorphinan	Dextrorphan→Dextrorphan-*O*-Glucuronide (without 2% BSA)	Dextrorphan→Dextrorphan-*O*-Glucuronide (with 2% BSA)
V_{max} (nmol · min^{-1} · mg MP^{-1})	0.066 ± 0.001	0.80 ± 0.24	2.0 ± 0.2	2.3 ± 0.4
K_M (μM)	5.0 ± 3.1	910 ± 500	690 ± 140	210 ± 110
Substrate $f_{u,mic}$	0.93 ± 0.10	1.0 ± 0.04	1.0 ± 0.04	0.88 ± 0.05
Cl_i (μl · min^{-1} · mg MP^{-1})	13	0.88	2.9	11
$Cl_{i,u}$ (μl · min^{-1} · mg MP^{-1})	14	0.95	2.9	12
Substrate plasma f_u	0.72 ± 0.07	0.55 ± 0.03	0.55 ± 0.03	0.55 ± 0.03

TABLE 2

The observed and predicted AUC_m/AUC_p values for the dextrorphan/dextromethorphan, 5OH-omeprazole/omeprazole, and omeprazole sulfone/omeprazole metabolite/parent pairs

The in vitro system used to determine the formation and elimination clearances, the predicted AUC_m/AUC_p for each pair using eqs. 6 and 7, and the AUC_m/AUC_p predicted/observed ratio are listed.

Parent	Metabolite	Observed AUC_m/AUC_p (Range)	In Vitro System	Equation Used	Predicted AUC_m/AUC_p	Predicted/Observed (Range)
Dextromethorphan	Dextrorphan	0.61 (0.52–0.70)	Pooled HLM	6	2.3	3.8 (3.3–4.4)
				7	1.3	2.1 (1.9–2.5)
Omeprazole	5OH-Omeprazole	0.48 (0.24–0.74)	Hepatocytes	6	0.37	0.78 (0.50–1.5)
				7	0.36	0.75 (0.49–1.5)
Omeprazole	Omeprazole sulfone	0.85 (0.79–0.94)	Pooled HLM	6	2.8	3.3 (3.0–3.5)
				7	2.6	3.1 (2.8–3.3)
			Hepatocytes	6	0.90	1.1 (0.96–1.2)
				7	0.90	1.1 (0.96–1.2)

zole is not available, the depletion clearances of these metabolites were measured instead of specific secondary metabolite formation clearance. The K_M and V_{max} for the formation of 5OH-omeprazole and omeprazole sulfone from omeprazole, as well as the depletion of these two metabolites in HLM, is shown in Fig. 4. The kinetic parameters for 5OH-omeprazole and omeprazole sulfone formation and depletion in HLM and human hepatocytes are summarized in Table 3. In pooled HLM, the unbound formation and depletion clearances for omeprazole sulfone were 7.7 and 35 $\mu l \cdot min^{-1} \cdot mg\ MP^{-1}$, respectively, demonstrating that the clearance of omeprazole sulfone is 5 times faster than its formation. Likewise, in human hepatocytes (Fig. 5), the elimination clearance of omeprazole sulfone ($Cl_{i,dep}$ = 48 ± 6 $\mu l \cdot h^{-1} \cdot 10^6\ cells^{-1}$) was approximately 13 times faster than the formation of omeprazole sulfone ($Cl_{i,f}$ = 3.6 ± 0.5 $\mu l \cdot h^{-1} \cdot 10^6\ cells^{-1}$).

The unbound formation clearance for 5OH-omeprazole in HLM was 8.2 $\mu l \cdot min^{-1} \cdot mg\ MP^{-1}$, but no depletion of 5OH-omeprazole was observed in pooled HLM (Fig. 4), and the percentage remaining of 5OH-omeprazole at 30 and 60 min when incubated with and without NADPH was similar. Because the in vitro-to-in vivo predictions of 5OH-omeprazole exposure suggested that 5OH-omeprazole is metabolically cleared, but no depletion of 5OH-omeprazole could be observed in pooled HLM, the depletion of 5OH-omeprazole was studied in cultured human hepatocytes (Fig. 5). Unlike in HLM, depletion of 5OH-omeprazole was detected in plated human hepatocytes. The $Cl_{i,f}$ for 5OH-omeprazole was 55 ± 2 $\mu l \cdot h^{-1} \cdot 10^6\ cells^{-1}$, and the $Cl_{i,dep}$ for 5OH-omeprazole was 100 ± 20 $\mu l \cdot h^{-1} \cdot 10^6\ cells^{-1}$.

Prediction of In Vivo 5OH-Omeprazole/Omeprazole and Omeprazole Sulfone/Omeprazole AUC_m/AUC_p. The in vivo AUC_m/AUC_p was predicted from only hepatocyte data for the 5OH-omeprazole/omeprazole pair and from both in vitro pooled HLM and hepatocyte data for the omeprazole sulfone/omeprazole pair. The AUC_m/AUC_p was predicted using eqs. 6 and 7 and compared with in vivo reported values. The predicted AUC_m/AUC_p values are summarized in Table 2, together with the average reported in vivo AUC_m/AUC_p values. Similar predicted AUC_m/AUC_p values were obtained using eqs. 6 and 7 (Table 2). On the basis of hepatocyte data, both the omeprazole sulfone/omeprazole and the 5OH-omeprazole/omeprazole AUC_m/AUC_p were predicted within 25% of the observed average AUC ratio, and the predicted ratio was within the observed range of the AUC ratios reported in different studies. Using HLM data, the AUC_m/AUC_p for omeprazole sulfone/omeprazole was overpredicted by 3-fold, on average.

Simulation of the Effect of Altered Formation or Elimination Clearance on In Vivo AUC_m/AUC_p. To determine whether altered metabolism of the probe metabolite affects the interpretation of in vivo AUC_m/AUC_p, the changes in a generic metabolite/parent AUC_m/AUC_p as a result of induction or inhibition of the formation and/or elimination of the metabolite were simulated (Fig. 6). The simulations

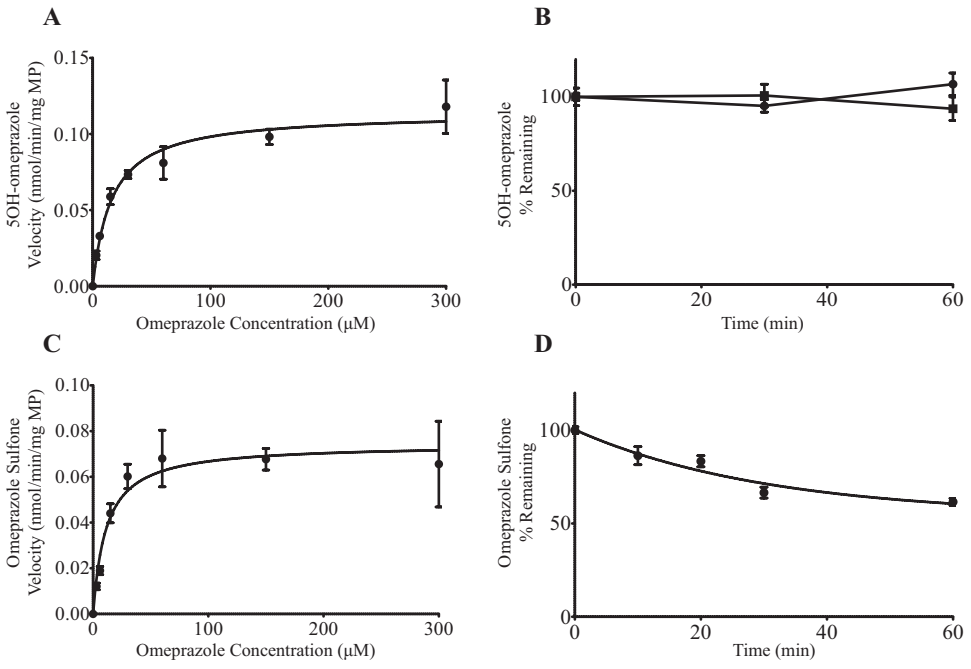

FIG. 4. Characterization of in vitro formation and depletion of 5OH-omeprazole and omeprazole sulfone in pooled HLM. Formation (A) and depletion (B) of 5OH-omeprazole. Formation (C) and depletion (D) of omeprazole sulfone. B, the percentage remaining of 5OH-omeprazole over time is provided with (■) and without (●) NADPH. Error bars represent the S.D. of three measurements.

TABLE 3

Kinetic characterization of 5OH-omeprazole and omeprazole sulfone formation and elimination in human liver microsomes and human hepatocytes

The Michaelis-Menten constants for the formation of 5OH-omeprazole and omeprazole sulfone from omeparazole in HLM are shown together with the depletion clearance of omeprazole sulfone in HLM. For hepatocytes, the formation and depletion clearances of 5OH-omeprazole and omeprazole sulfone are listed. The unbound fractions of each substrate in pooled HLM and plasma are also listed.

	Omeprazole→ 5OH-Omeprazole	Omeprazole→Omeprazole Sulfone	5OH-Omeprazole Depletion	Omeprazole Sulfone Depletion
V_{max} (nmol · min^{-1} · mg MP^{-1})	0.11 ± 0.01	0.074 ± 0.007	ND	ND
K_M (μM)	16 ± 5	11 ± 5	ND	ND
Substrate $f_{u,mic}$	0.86 ± 0.04	0.86 ± 0.04	0.84 ± 0.04	0.92 ± 0.03
Cl_i (μl · min^{-1} · mg MP^{-1})	7.1	6.6	No depletion	32 ± 4
$Cl_{i,u}$ (μl · min^{-1} · mg MP^{-1})	8.2	7.7	No depletion	35
Hepatocyte $Cl_{i,u}$ (μl · h^{-1} · 10^6 cells^{-1})	55 ± 2	3.6 ± 0.5	100 ± 20	48 ± 6
Substrate plasma f_u	0.061 ± 0.014	0.061 ± 0.014	0.092 ± 0.033	0.0048 ± 0.029

ND, value was not determined.

were conducted assuming sequential metabolism of the metabolite before reaching the systemic circulation is possible (eq. 7). Induction or inhibition of the formation of the metabolite resulted in an increase or decrease in AUC_m/AUC_p, respectively, when the elimination of the metabolite was not entirely mediated by the same enzyme that forms the metabolite (metabolite's $f_{m,E1} < 1$; Fig. 6). This effect was attenuated when the metabolite was cleared partly by the same enzyme that forms it, and no change in the AUC_m/AUC_p was observed when the metabolite was entirely eliminated by the same enzyme that forms it. Induction or inhibition of the elimination of the metabolite by E2 resulted in a decrease or increase in AUC_m/AUC_p, respectively. This effect was most pronounced when $f_{m,E2}$ for the metabolite approached unity. The simulations show that on the basis of just observed in vivo AUC_m/AUC_p data, it is extremely difficult to determine whether metabolite formation or elimination pathways are affected unless the elimination pathways of the metabolite are characterized and measured.

Discussion

The data obtained in this study show that in vivo AUC_m/AUC_p can be accurately predicted from in vitro data using only primary metabolite formation and depletion kinetics. Comparison of the predicted and observed AUC_m/AUC_p for a given metabolite allows determination of the importance of hepatic metabolic clearance in the elimination of that metabolite as shown for omeprazole and dextromethorphan metabolite AUC_m/AUC_p. On the other hand, the overprediction of AUC_m/AUC_p can be used as an indication of missing/unidentified elimination pathways of the metabolite. Such information could be useful during drug development for compounds whose elimination has not been completely characterized but preliminary in vivo concentration data are available, as can be the case when a candidate compound is tested for a new target.

Although the dextrorphan/dextromethorphan AUC_m/AUC_p was predicted within 2.1-fold using HLM data alone, based on the predictions with 5OH-omeprazole and omeprazole sulfone, use of hepatocytes is more reliable for metabolite depletion studies than HLM. Based on the in vitro formation clearances, glucuronidation is the major elimination pathway for dextrorphan. In this study, dextrorphan-*O*-glucuronide formation measured in the presence of 2% BSA was 12-fold more efficient than the formation of 3-hydroxymorphinan. The overall prediction accuracy suggests that the major elimination pathways of dextrorphan are accounted for via glucuronidation and 3-hydroxymorphinan formation. UGT2B isoforms were found to be responsible for dextrorphan glucuronidation, similar to related

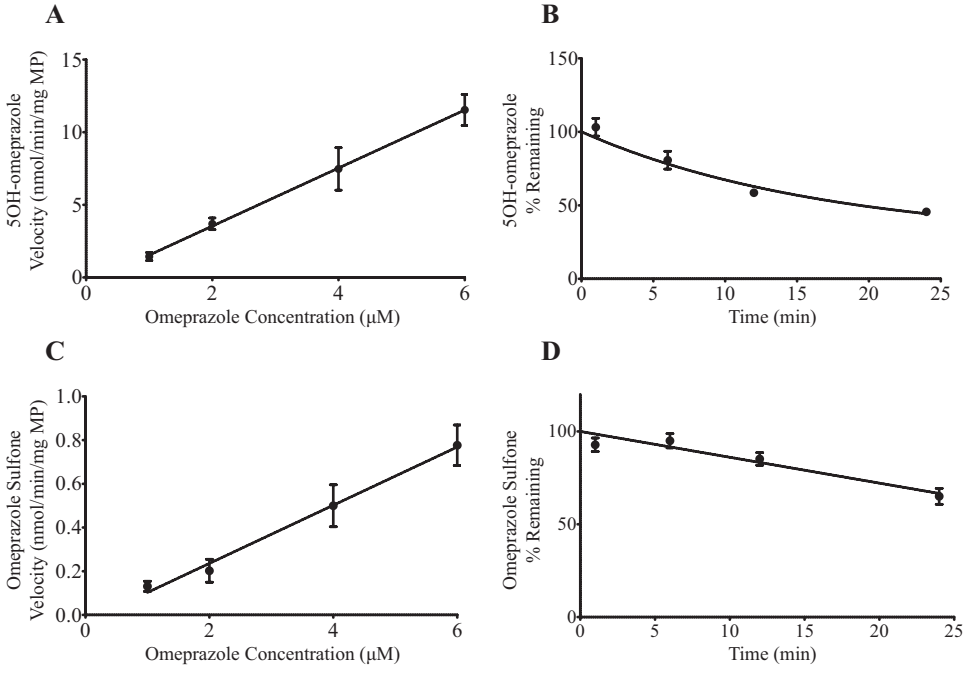

FIG. 5. Characterization of in vitro formation and depletion of 5OH-omeprazole and omeprazole sulfone in hepatocytes. Formation of 5OH-omeprazole (A) and omeprazole sulfone (C) from omeprazole. The percentage remaining of 5OH-omeprazole (B) and omeprazole sulfone (D). Error bars represent the S.D. of four measurements.

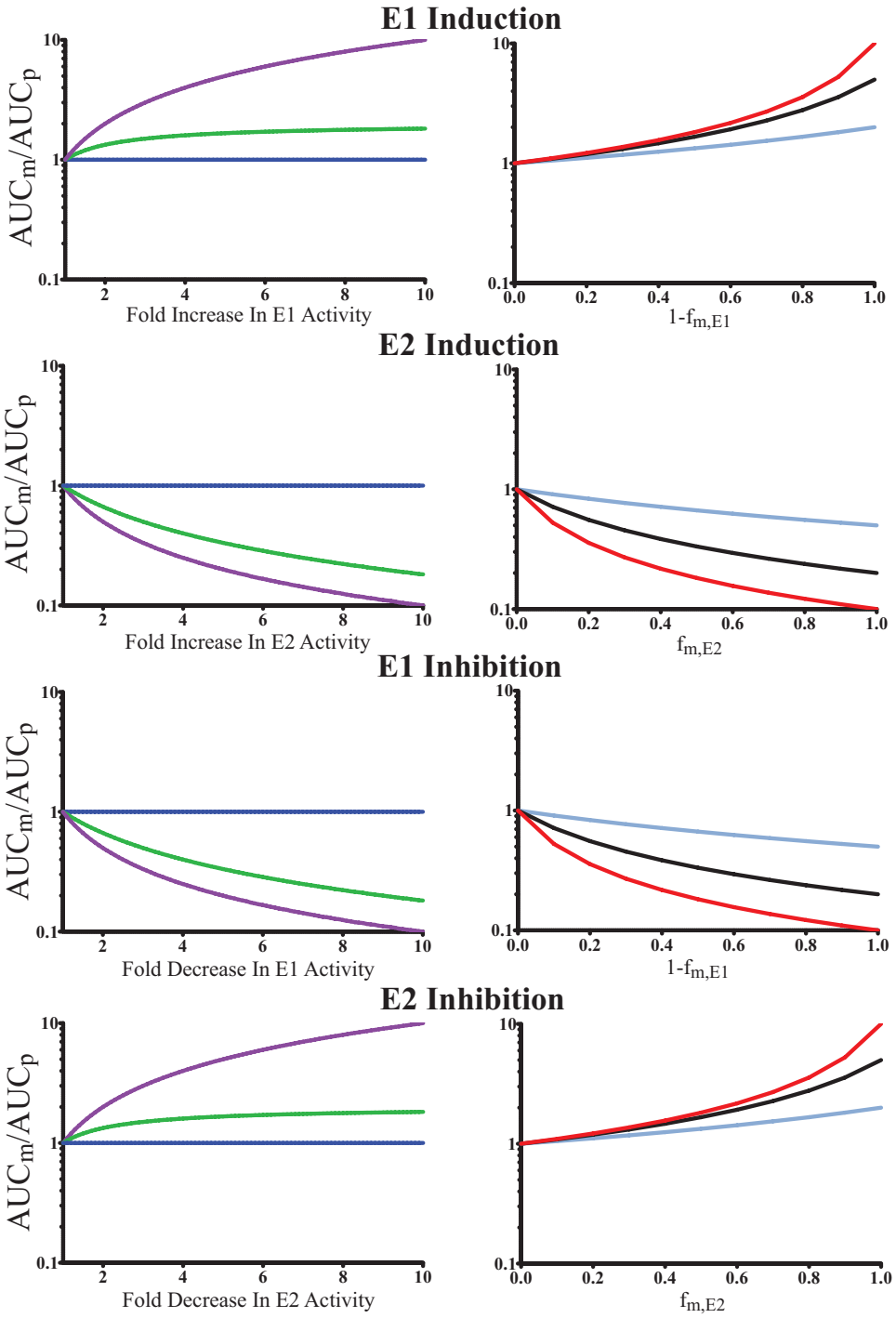

FIG. 6. Simulation of the effects of inhibition and induction of probe metabolite clearance in vivo on AUC_m/AUC_p activity measures. The AUC_m/AUC_p for a generic metabolite/parent pair in which E1 is solely responsible for forming the probe metabolite and the probe metabolite is eliminated by enzymes E1 and E2 as described under *Materials and Methods* is simulated under the conditions of E1 induction, E2 induction, E1 inhibition, and E2 inhibition. Left, the condition in which E1 is the only enzyme that clears the metabolite ($f_{m,E1} = 1$ and $f_{m,E2} = 0$ for metabolite elimination) is shown as the dark blue line, the condition in which both E1 and E2 have equal responsibility for clearing the metabolite ($f_{m,E1} = 0.5$ and $f_{m,E2} = 0.5$) is shown as the green line, and the condition in which E2 is the only enzyme that clears the metabolite ($f_{m,E1} = 0$ and $f_{m,E2} = 1$) is shown as the purple line. Right, the effect of $f_{m,E1}$ (the fraction of the metabolite clearance by the same enzyme which forms it) on the magnitude of change in AUC_m/AUC_p after a 2-fold (light blue line), 5-fold (black line), and 10-fold (red line) increase (for induction) or decrease (for inhibition) in the specified enzyme activity.

opioids morphine and codeine (Court et al., 2003). Dextrorphan glucuronidation has been previously reported in vitro and in vivo (Duché et al., 1993; Takashima et al., 2005; Abduljalil et al., 2010), but formation kinetics have not been characterized. Overall, the kinetic values determined for dextrorphan and 3-hydroxymorphinan formation were similar to those reported previously (Kerry et al., 1994). The values determined for glucuronidation in the presence of 2% BSA are likely appropriate for clearance predictions because BSA increases glucuronidation efficiency in HLM by binding fatty acids that inhibit UGTs (Kilford et al., 2009). The difference in the prediction accuracy between eqs. 6 and 7 (3.8- and 2.1-fold, respectively) reflects the fact that the dextrorphan extraction ratio is predicted to be high and, hence, sequential metabolism of dextrorphan in the liver is likely. The remaining 2.1-fold overprediction in the AUC_m/AUC_p is likely due to extrahepatic glucuronidation of dextrorphan rather than unaccounted renal clearance. UGT2B enzymes are expressed in many extrahepatic tissues (Nakamura et al., 2008), and dextrorphan undergoes only minor renal elimination relative to predicted total metabolic clearance (4.5 versus 38.7 l/h) (Duché et al., 1993; Abduljalil et al., 2010).

The fact that in vivo AUC_m/AUC_p for 5OH-omeprazole/omeprazole and omeprazole sulfone/omeprazole could be accurately predicted from hepatocyte primary metabolite $Cl_{i,dep}$ suggests that, to predict the exposure of primary metabolites, secondary metabolic

pathways do not need to be identified. This is useful for metabolites such as 5OH-omeprazole and omeprazole sulfone that appear to undergo metabolism to multiple sequential species. The measured $Cl_{i,f}$ for 5OH-omeprazole and omeprazole sulfone are in agreement with previously determined values in HLM (Andersson et al., 1993). The $Cl_{i,dep}$ of omeprazole sulfone (32 $\mu l \cdot min^{-1} \cdot mg\ MP^{-1}$) was greater than the previously measured $Cl_{i,f}$ of 5-hydroxyomeprazole sulfone from omeprazole sulfone (9.7 $\mu l \cdot min^{-1} \cdot mg\ MP^{-1}$), suggesting a contribution of additional pathways to omeprazole sulfone elimination. The reason for a better prediction of the in vivo omeprazole sulfone/omeprazole AUC_m/AUC_p from hepatocyte data than from HLM data could be due to a more accurate prediction of both the formation and elimination clearance of omeprazole sulfone from hepatocytes than from HLM, but in vivo data of clearance of omeprazole sulfone would be needed to determine this. It is noteworthy that because omeprazole sulfone is 12.7-fold more bound in plasma than omeprazole (Table 3), the unbound AUC_m/AUC_p of omeprazole sulfone/omeprazole is 0.067, whereas the observed total AUC_m/AUC_p is 0.85 (Table 2). This shows that when AUC_m/AUC_p ratios are used to predict the importance of metabolites in pharmacologic activity, the difference between the plasma f_u for the metabolite and parent should be considered together with the AUC_m/AUC_p.

The AUC_m/AUC_p for 5OH-omeprazole/omeprazole could not be predicted from HLM data because of the lack of measurable depletion of 5OH-omeprazole. Based on the reported formation kinetics of 5-hydroxyomeprazole sulfone from 5OH-omeprazole (Andersson et al., 1994), 0.5% depletion is expected in HLM (0.1 mg/ml) after a 60-min incubation. This is not sufficient to obtain depletion kinetic estimates. 5OH-omeprazole and carboxyomeprazole are the major metabolites detected in urine after omeprazole administration (Renberg et al., 1989), and sequential formation of carboxyomeprazole from omeprazole aldehyde is likely responsible for the majority of 5OH-omeprazole depletion in hepatocytes. It is likely that alcohol dehydrogenases (ADHs) and aldehyde dehydrogenases form omeprazole aldehyde and carboxylic acid in human hepatocytes because the ADH isoforms that metabolize xenobiotics are localized in the cytosol and expressed in the liver (Crabb et al., 2004). Because ADH enzymes are induced by ethanol (Kawashima et al., 1996; Crabb et al., 2004), their activity is expected to vary between individuals. This may explain the considerable variability (up to 10-fold) observed in the AUC_m/AUC_p of 5OH-omeprazole/omeprazole between reported in vivo studies even after controlling for CYP2C19 genotype (Tassaneeyakul et al., 2000; Shirai et al., 2001).

Metabolite ratios or specific metabolite formation measures are usually considered more sensitive measures than the AUC_p to determine inhibition or induction of specific P450 enzymes. This is especially the case for probe drugs that undergo metabolism by multiple P450s, for which use of a specific metabolite measure rather than AUC_p is necessary. Thus, altered AUC_m/AUC_p (or C_m/C_p) of the probe metabolite will usually be considered as indication of an interaction even in the absence of effect on AUC_p. For example, an increase in AUC_m/AUC_p could be interpreted as weak in vivo induction of Cl_f when the drug-drug interaction was, in fact, due to inhibition of Cl_m as shown by the simulations. In practice, this is illustrated when CYP2C19 poor metabolizer genotype, likely decreasing the CYP2C19-mediated elimination of omeprazole sulfone, causes an increased omeprazole sulfone/omeprazole AUC_m/AUC_p, the probe measure for CYP3A4 (Yang et al., 2009; Tu et al., 2010). For the dextrorphan/dextromethorphan and 5OH-omeprazole/omeprazole ratios, it is unlikely that major changes in secondary pathways would be misinterpreted if AUC_p is measured in the study. However, if the change in the metabolic ratio is weak (suggesting that no effect in the less sensitive AUC_p measure would be expected) or only a single time point ratio is measured, the possibility of misinterpretation is high. The challenge of identifying the correct interpretation of AUC_m/AUC_p ratios is emphasized by the simulations that show that induction of metabolite clearance has an identical effect on the AUC_m/AUC_p as inhibition of the formation of the metabolite. In addition, the simulations show that the sensitivity of the metabolic ratio is greatly dampened if the metabolite clearance is partially mediated by the same enzyme as the formation, with no effect on the ratio if the same enzyme forms and eliminates the metabolite. These results warrant more thorough characterization of the complete formation and elimination clearances of the metabolites (including sequential metabolites) in drug-drug interaction studies. For dextrorphan, treatment of samples with β-glucuronidase or measurement of the dextrorphan glucuronide should be considered when CYP2D6 activity is measured.

In this study, in vitro-to-in vivo predictions of AUC_m/AUC_p were used to determine the importance of secondary metabolism in 5OH-omeprazole and dextrorphan clearance, and the major in vivo metabolic pathways were predicted. The results show that in vitro-to-in vivo predictions of metabolite exposure are a valuable tool for improving our understanding of P450 probes and metabolite clearance pathways and for predicting relative metabolite exposures after administration of parent drug. Kinetic characterization of the metabolism of dextrorphan and 5OH-omeprazole afforded accurate prediction of AUC_m/AUC_p, demonstrating that in vivo metabolite disposition (relative to parent) can be predicted from in vitro data. The results obtained in this study emphasize the significance of understanding the secondary metabolic processes involved in elimination of metabolites used as in vivo P450 activity measures.

Acknowledgments

We thank Dr. Leslie Dickmann (Amgen Incorporated, Seattle, WA) for the generous donation of plated human hepatocytes. We also thank Drs. Thomas Baillie, Duane Bloedow, and R. Scott Obach for helpful discussions during this work.

Authorship Contributions

Participated in research design: Lutz and Isoherranen.
Conducted experiments: Lutz.
Performed data analysis: Lutz and Isoherranen.
Wrote or contributed to the writing of the manuscript: Lutz and Isoherranen.

References

Abdul Manap R, Wright CE, Gregory A, Rostami-Hodjegan A, Meller ST, Kelm GR, Lennard MS, Tucker GT, and Morice AH (1999) The antitussive effect of dextromethorphan in relation to CYP2D6 activity. *Br J Clin Pharmacol* **48:**382–387.

Abduljalil K, Frank D, Gaedigk A, Klaassen T, Tomalik-Scharte D, Jetter A, Jaehde U, Kirchheiner J, and Fuhr U (2010) Assessment of activity levels for CYP2D6*1, CYP2D6*2, and CYP2D6*41 genes by population pharmacokinetics of dextromethorphan. *Clin Pharmacol Ther* **88:**643–651.

Anderson S, Luffer-Atlas D, and Knadler MP (2009) Predicting circulating human metabolites: how good are we? *Chem Res Toxicol* **22:**243–256.

Andersson T, Miners JO, Veronese ME, Tassaneeyakul W, Tassaneeyakul W, Meyer UA, and Birkett DJ (1993) Identification of human liver cytochrome P450 isoforms mediating omeprazole metabolism. *Br J Clin Pharmacol* **36:**521–530.

Andersson T, Miners JO, Veronese ME, and Birkett DJ (1994) Identification of human liver cytochrome P450 isoforms mediating secondary omeprazole metabolism. *Br J Clin Pharmacol* **37:**597–604.

Angiolillo DJ, Gibson CM, Cheng S, Ollier C, Nicolas O, Bergougnan L, Perrin L, LaCreta FP, Hurbin F, and Dubar M (2011) Differential effects of omeprazole and pantoprazole on the pharmacodynamics and pharmacokinetics of clopidogrel in healthy subjects: randomized, placebo-controlled, crossover comparison studies. *Clin Pharmacol Ther* **89:**65–74.

Bertilsson L, Tybring G, Widén J, Chang M, and Tomson T (1997) Carbamazepine treatment induces the CYP3A4 catalysed sulphoxidation of omeprazole, but has no or less effect on hydroxylation via CYP2C19. *Br J Clin Pharmacol* **44:**186–189.

Böttiger Y, Tybring G, Götharson E, and Bertilsson L (1997) Inhibition of the sulfoxidation of omeprazole by ketoconazole in poor and extensive metabolizers of S-mephenytoin. *Clin Pharmacol Ther* **62:**384–391.

Court MH, Krishnaswamy S, Hao Q, Duan SX, Patten CJ, Von Moltke LL, and Greenblatt DJ (2003) Evaluation of 3′-azido-3′-deoxythymidine, morphine and codeine as probe substrates

for UDP-glucuronosyltransferase 2B7 (UGT2B7) in human liver microsomes: specificity and influence of the UGT2B7*2 polymorphism. *Drug Metab Dispos* **31:**1125–1133.
Crabb DW, Matsumoto M, Chang D, and You M (2004) Overview of the role of alcohol dehydrogenase and aldehyde dehydrogenase and their variants in the genesis of alcohol-related pathology. *Proc Nutr Soc* **63:**49–63.
Duché JC, Quérol-Ferrer V, Barré J, Mésangeau M, and Tillement JP (1993) Dextromethorphan O-demethylation and dextrorphan glucuronidation in a French population. *Int J Clin Pharmacol Ther Toxicol* **31:**392–398.
Fitzgerald LW, Burn TC, Brown BS, Patterson JP, Corjay MH, Valentine PA, Sun JH, Link JR, Abbaszade I, Hollis JM, et al. (2000) Possible role of valvular serotonin 5-HT_{2B} receptors in the cardiopathy associated with fenfluramine. *Mol Pharmacol* **57:**75–81.
Ho PC, Abbott FS, Zanger UM, and Chang TK (2003) Influence of CYP2C9 genotypes on the formation of a hepatotoxic metabolite of valproic acid in human liver microsomes. *Pharmacogenomics J* **3:**335–342.
Jones DR, Gorski JC, Haehner BD, O'Mara EM Jr, and Hall SD (1996) Determination of cytochrome P450 3A4/5 activity *in vivo* with dextromethorphan N-demethylation. *Clin Pharmacol Ther* **60:**374–384.
Kawashima O, Yamauchi M, Maezawa Y, and Toda G (1996) Effects of cimetidine on blood ethanol levels after alcohol ingestion and genetic polymorphisms of sigma-alcohol dehydrogenase in Japanese. *Alchol Clin Exp Res* **20 (1 Suppl):**36A–39A.
Kerry NL, Somogyi AA, Bochner F, and Mikus G (1994) The role of CYP2D6 in primary and secondary oxidative metabolism of dextromethorphan: *in vitro* studies using human liver microsomes. *Br J Clin Pharmacol* **38:**243–248.
Kilford PJ, Stringer R, Sohal B, Houston JB, and Galetin A (2009) Prediction of drug clearance by glucuronidation from *in vitro* data: use of combined cytochrome P450 and UDP-glucuronosyltransferase cofactors in alamethicin-activated human liver microsomes. *Drug Metab Dispos* **37:**82–89.
Leclercq L, Cuyckens F, Mannens GS, de Vries R, Timmerman P, and Evans DC (2009) Which human metabolites have we MIST? Retrospective analysis, practical aspects, and perspectives for metabolite identification and quantification in pharmaceutical development. *Chem Res Toxicol* **22:**280–293.
Levy RH, Lane EA, Guyot M, Brachet-Liermain A, Cenraud B, and Loiseau P (1983) Analysis of parent drug-metabolite relationship in the presence of an inducer. Application to the carbamazepine-clobazam interaction in normal man. *Drug Metab Dispos* **11:**286–292.
Lutz JD, Fujioka Y, and Isoherranen N (2010) Rationalization and prediction of *in vivo* metabolite exposures: the role of metabolite kinetics, clearance predictions and *in vitro* parameters. *Expert Opin Drug Metab Toxicol* **6:**1095–1109.
Nakamura A, Nakajima M, Yamanaka H, Fujiwara R, and Yokoi T (2008) Expression of UGT1A and UGT2B mRNA in human normal tissues and various cell lines. *Drug Metab Dispos* **36:**1461–1464.
Nakashima D, Takama H, Ogasawara Y, Kawakami T, Nishitoba T, Hoshi S, Uchida E, and Tanaka H (2007) Effect of cinacalcet hydrochloride, a new calcimimetic agent, on the pharmacokinetics of dextromethorphan: *in vitro* and clinical studies. *J Clin Pharmacol* **47:**1311–1319.
Pang KS and Gillette JR (1979) Sequential first-pass elimination of a metabolite derived from a precursor. *J Pharmacokinet Biopharm* **7:**275–290.
Reese MJ, Wurm RM, Muir KT, Generaux GT, St John-Williams L, and McConn DJ (2008) An *in vitro* mechanistic study to elucidate the desipramine/bupropion clinical drug-drug interaction. *Drug Metab Dispos* **36:**1198–1201.
Renberg L, Simonsson R, and Hoffmann KJ (1989) Identification of two main urinary metabolites of [14C]-omeprazole in humans. *Drug Metab Dispos* **17:**69–76.
Riss J, Cloyd J, Gates J, and Collins S (2008) Benzodiazepines in epilepsy: pharmacology and pharmacokinetics. *Acta Neurol Scand* **118:**69–86.
Shirai N, Furuta T, Moriyama Y, Okochi H, Kobayashi K, Takashima M, Xiao F, Kosuge K, Nakagawa K, Hanai H, et al. (2001) Effects of CYP2C19 genotypic differences in the metabolism of omeprazole and rabeprazole on intragastric pH. *Ailment Pharmacol Ther* **15:**1929–1937.
Streetman DS, Bertino JS Jr, and Nafziger AN (2000) Phenotyping of drug-metabolizing enzymes in adults: a review of in-vivo cytochrome P450 phenotyping probes. *Pharmacogenetics* **10:**187–216.
Takashima T, Murase S, Iwasaki K, and Shimada K (2005) Evaluation of dextromethorphan metabolism using hepatocytes from CYP2D6 poor and extensive metabolizers. *Drug Metab Pharmacokinet* **20:**177–182.
Tassaneeyakul W, Vannaprasaht S, and Yamazoe Y (2000) Formation of omeprazole sulphone but not 5-hydroxyomeprazole is inhibited by grapefruit juice. *Br J Clin Pharmacol* **49:**139–144.
Templeton IE, Thummel KE, Kharasch ED, Kunze KL, Hoffer C, Nelson WL, and Isoherranen N (2008) Contribution of itraconazole metabolites to inhibition of CYP3A4 *in vivo*. *Clin Pharmacol Ther* **83:**77–85.
Tu JH, Hu DL, Dai LL, Sun Y, Fan L, Zhang M, Tan ZR, Chen Y, Li Z, and Zhou HH (2010) Effect of glycyrrhizin on CYP2C19 and CYP3A4 activity in healthy volunteers with different CYP2C19 genotypes. *Xenobiotica* **40:**393–399.
Yang LJ, Fan L, Liu ZQ, Mao YM, Guo D, Liu LH, Tan ZR, Peng L, Han CT, Hu DL, et al. (2009) Effects of allicin on CYP2C19 and CYP3A4 activity in healthy volunteers with different CYP2C19 genotypes. *Eur J Clin Pharmacol* **65:**601–608.
Yeh GC, Tao PL, Ho HO, Lee YJ, Chen JY, and Sheu MT (2003) Analysis of pharmacokinetic parameters for assessment of dextromethorphan metabolic phenotypes. *J Biomed Sci* **10:**552–564.
Yeung CK, Fujioka Y, Hachad H, Levy RH, and Isoherranen N (2011) Are circulating metabolites important in drug-drug interactions?: Quantitative analysis of risk prediction and inhibitory potency. *Clin Pharmacol Ther* **89:**105–113.
Yu A and Haining RL (2001) Comparative contribution to dextromethorphan metabolism by cytochrome P450 isoforms in vitro: can dextromethorphan be used as a dual probe for both CYP2D6 and CYP3A activities? *Drug Metab Dispos* **29:**1514–1520.

Address correspondence to: Dr. Nina Isoherranen, School of Pharmacy, Department of Pharmaceutics, University of Washington, Box 357610, H272 Health Science Building, Seattle, WA 98195-7610. E-mail: ni2@u.washington.edu